CHEMISTRY OF MATERIALS

pubs.acs.org/cm

Article

Photo-Crosslinkable Polymeric Coatings Providing Chemically Versatile Reactive Surfaces on Various Substrates

Seungyeon Choi, Lane D. Yutzy, Yun Hee Ko, Jin-Kyun Lee, Jangwook P. Jung,* and Myungwoong Kim*

Cite This: https://doi.org/10.1021/acs.chemmater.3c00225

Read Online

ACCESS | Metrics & More | Article Recommendations | Supporting Information

ABSTRACT: We demonstrate a chemical route to attain simple, clean, scalable, photopatternable, chemically adjustable, and versatile systems to fabricate reactive organic thin films. Their surfaces exhibit effective biocompatibility, controlled reactivity, and processability on various surface types, i.e., photo-crosslinkable polymeric thin films with various functionalities, further applicable for the definition of surface activity for interfacing biological objects. The copolymers were synthesized with three monomers: a poly(ethylene glycol)-containing monomer, a monomer releasing a primary amine upon exposure to UV light, and a monomer bearing cyclic dithiocarbonate or glycidyl groups that are highly reactive with the amine. The resulting copolymers were processed with polar solvents such as water or alcohol for coating and were readily crosslinked under UV light illumination to form a highly stable molecular network, beneficial for defining selective reactive surfaces in a desired region on a variety of organic and inorganic substrates. The designed system was chemically versatile in immobilizing biologically relevant molecules on the surfaces by (i) post-crosslinking modification through the reaction of bovine serum albumin on the remaining surface reactive group with a primary amine in the protein and (ii) pre-crosslinking formulation with reactive gelatin that has the functionality to crosslink in the composite thin film. We further showed that the resulting coating on a glass or polystyrene substrate provided excellent biocompatibility and growth of C2C12 murine myocytes.

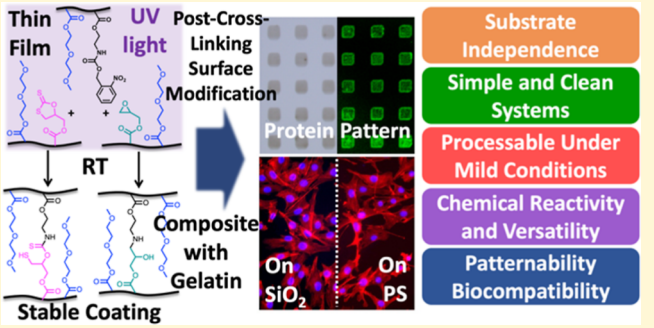

INTRODUCTION

Engineering the surface properties of materials for a targeted application is crucial for them to attain their desired functions and, hence, requires precise molecular engineering skills. For example, selective immobilization of biomaterials, including oligopeptides and engineered proteins, is considered a versatile tool to understand the behaviors of cells on 2D or in 3D materials.[1−4] Specifically, in the case of 2D cell culture, it is important to create an engineered surface to modulate the interactions between cells and the surface.[5,6] Another example is material surface patterning at the micro- or nanometer scale, which requires significant engineering of the molecular architecture of materials[7,8] to enable the manufacturing of almost all electronic devices with a photolithographic tool to fabricate integrated circuits.[9] The fine control of surface energy enables the regulation of the self-assembly behaviors of block copolymer chains to form nano-sized domains with desired orientation and alignment.[10−12]

Surfaces derived from synthetic coating materials with molecular-level design have been extensively investigated to facilitate the modulation of material functions. Many strategies have been proposed, which include forming self-assembled monolayers[13,14] or polymer brushes,[15,16] plasma treatment and subsequent chemical modification,[17−20] and the formation of an organic functional polymer thin film coated on the surface.[21,22] In particular, the approach using polymer coating has attracted scientific and technological attention. Beyond its ease of the process, it can be designed at the molecular level to attain well-controlled functionality, enabling the aforementioned different and significant functions, in which surface properties, such as surface energy, wettability, and surface chemical cues, are important.[23,24] This type of organic coating should meet the requirements for specific applications to expand its applicability to different fields. First, the coating material should be processable onto chemically dissimilar surfaces, including inorganic and organic materials, under mild conditions to achieve substrate independence. For example, in biological/biomedical engineering, polystyrene (PS) is a widely utilizable polymeric material for two-dimensional cell culture

Received: February 1, 2023
Revised: April 10, 2023

Scheme 1. RAFT Copolymerization for Synthesizing (a) Poly(PEGMEMA-*r*-GMA) (MG), (b) Poly(PEGMEMA-*r*-NBOCAEMA) (MN), and (c) Poly(PEGMEMA-*r*-DTCMMA) (MD)

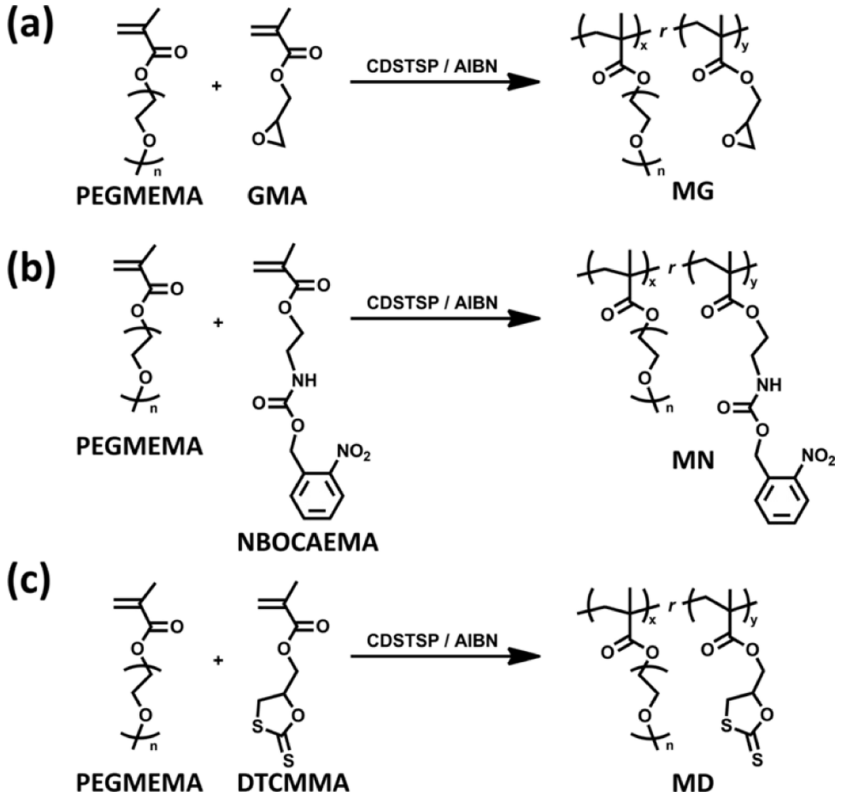

owing to its outstanding light transmittance, mechanical properties, and commercial availability.[25] However, its poor chemical resistance and low T_g (≈100 °C) heavily limit the processing with organic solvents and under high-temperature conditions to form thermally crosslinked coatings.[26−28] Typically, culture surfaces of PS are treated with oxygen plasma to increase hydrophilicity; however, this is far less functional than any other direct functionalization or conjugation methods. Fabricating extracellular matrix (ECM) coatings or poly(lysine) coatings on PS surfaces can make this possible, although the deposition processes are highly dependent on the surface energy of the PS surface, requiring more complicated processes with different materials and treatments. Second, chemical versatility is required for defining desired functionalities toward target functions with functionalization routes that can be performed under mild conditions so that the underlying material is intact; hence, its properties are not lost. Third, the material system should be utilized in complex composite systems to expand its potential for different applications.

Herein, to simultaneously overcome all challenges, we demonstrate photo-crosslinkable copolymers that can be coated onto various surfaces and also present controlled functionalities enabling surface-active functions. Three types of copolymers were synthesized by reversible addition−fragmentation chain transfer (RAFT) copolymerization of poly(ethylene glycol) methyl ether methacrylate (PEGMEMA) with (i) 2-((((2-nitrobenzyl)oxy)carbonyl)amino)ethyl methacrylate (NBOCAEMA) releasing a primary amine upon an exposure to UV light [poly(PEGMEMA-*r*-NBOCAEMA); MN],[29,30] or with (ii) glycidyl methacrylate (GMA) [poly(PEGMEMA-*r*-GMA); MG], or (iii) cyclic dithiocarbonate methylene methacrylate (DTCMMA) [poly(PEGMEMA-*r*-DTCMMA); MD] (Scheme 1). Released amines upon the deprotection of the *o*-nitrobenzyl group were highly effective to induce interchain crosslinking reactions with various ester functionalities in an assembled colloid and thin film geometries.[31,32] The reactive epoxide and cyclic dithiocarbonate rings also are expected to readily undergo the ring opening reaction with the primary amine released by UV light illumination,[33,34] making the crosslinking process under mild conditions feasible. Furthermore, due to the presence of highly polar PEG units in all copolymers, dual-component systems consisting of MN and MG or MN and MD were all processable with polar solvents, e.g., water and ethanol, and readily crosslinked simply by UV light illumination, which allows defining and stabilizing an active thin film surface in a desirable region by a photolithographic manner, without any additives and heating process. We further utilized the designed materials and resulting surfaces to attain surface activeness by incorporating biologically active macromolecules via two routes: (i) the resulting thin films were further modified with the reaction of bovine serum albumin (BSA) in the presence of the remaining surface reactive groups (epoxide and DTC); (ii) the copolymers were further mixed with fish skin gelatin bearing methacrylate[35,36] to form the composite thin film, further allowing additional crosslinking in the presence of a photo-radical generator. The amount of gelatin imparting surface-active functionality was also controllable without any degradation in the crosslinking capability. Composite thin films formed on glass and PS substrates were examined to assess the viability and growth of C2C12 murine myocytes.

https://doi.org/10.1021/acs.chemmater.3c00225
Chem. Mater. XXXX, XXX, XXX−XXX

MATERIALS AND METHODS

Materials. Potassium *tert*-butoxide (97%), 2-nitrobenzyl alcohol (97%), and 4-(dimethylamino)pyridine (DMAP; 99%) were purchased from Alfa Aesar. Lithium bromide (>99.0%), 2-isocyanatoethyl methacrylate (>98.0%), dibutyltin dilaurate (DBTL; >95.0%), and fluorescein isothiocyanate isomer I (FITC; >90%) were supplied by the Tokyo Chemical Industry Co., Ltd. Heptane (>98.0%), sodium sulfate (Na_2SO_4, >99.0%), ethyl acetate (99.5%), *n*-hexane (>95.0%), acetonitrile (>99.5%), and dimethyl sulfoxide (DMSO; 99.5%) were purchased from Daejung Chemicals & Metals Co., Ltd. Phosphate buffered saline (PBS; 10× solution, pH = 7.4 ± 0.1), dichloromethane (DCM; 99.5%), diethyl ether (99.0%), and ethanol (94.5%) were obtained from Samchun Chemicals. Tetrahydrofuran (THF; 99.9%), 1-dodecanethiol (>98.0%), carbon disulfide (CS_2; 99.9%), 1,4-dioxane (99.8%), sodium thiosulfate pentahydrate (>99.5%), 4,4′-azobis(4-cyanopentanoic acid) (>98.0%), PEGMEMA ($M_n \approx 300$), lithium phenyl-2,4,6-tirmethyl-benzoylphosphinate (LAP; >95%), albumin-FITC conjugate (FITC-labeled BSA), glycidyl methacrylate (GMA; 97%), and gelatin from cold water skin (fGel) were purchased from Sigma-Aldrich Co., Ltd. GMA and PEGMEMA were passed through a neutral aluminum oxide column to remove the inhibitor before polymerization. 2,2′-Azobis(2-methylpropionitrile) (AIBN) was purchased from Junsei Chemicals and recrystallized from methanol before use. Cyclic dithiocarbonate methylene methacrylate (DTCMMA), 2-((((2-nitrobenzyl)oxy)carbonyl)amino)ethyl methacrylate (NBOCAEMA), and 4-cyano-4-(dodecylsulfanylthiocarbonyl)sulfanyl pentanoic acid (CDSTSP) were synthesized by following previously reported procedures.[30,37,38]

General Procedure of Random Copolymerization. All copolymers were synthesized via RAFT polymerization. PEGMEMA (90.00 mmol) and the second monomer (22.50 mmol; NBOCAEMA for MN, DTCMMA for MD, or GMA for MG) were added to a Schlenk flask equipped with a stir bar. CDSTSP (1.80 mmol), AIBN (0.90 mmol), and 1,4-dioxane (50 wt %) were added to the monomer mixture. The feed ratio, i.e., $f_{PEGMEMA}$ and f_{GMA} (or $f_{NBOCAEMA}$ or f_{DTCMMA}), was 0.80 and 0.20, respectively. The resulting solution was subjected to three freeze−pump−thaw cycles to remove dissolved gases. Then, copolymerization was performed at 70 °C for 4 h for MG and MN and 1.5 h for MD. After the copolymerization, the resulting solution was cooled to room temperature and exposed to air. The solution was diluted with THF, followed by the addition to excess diethyl ether for precipitation. The resulting solid was collected by vacuum filtration and dried in a vacuum oven at room temperature.

Synthesis of Methacrylate-Incorporated Fish Skin Gelatin. Methacrylate-incorporated fish skin gelatin (fGelMA) was synthesized by the reaction of fGel with GMA.[36,39] Briefly, fGel (10.0 g) was dissolved in 100 mL of DMSO, followed by stirring at 50 °C for 30 min. To tune the degree of methacrylate incorporation from low to high, 1.218 g of GMA (or 8.529 g) and 0.175 g of DMAP (or 1.222 g) were added to the fGel solution, followed by stirring at 50 °C for 2 days. The resulting solution was purified through dialysis (3500 Da molecular weight cut-off) at 40 °C for 5 days. The resulting solution was lyophilized for 5 days. The degree of the addition reaction (DA) was quantified using proton nuclear magnetic resonance (^{1}H NMR) spectroscopy following the literature,[39] estimated to be 0.143 (or 0.920) for the reactions under two different reaction stoichiometries.

Photo-Crosslinking of Thin Films Consisting of Two Copolymers. Copolymer solutions (2.5 wt %) were prepared by dissolving MN and MD (or MG) in ethanol. The molar ratio of NBOC units in the MN and DTC units in MD (or GMA units in MG) was varied to 1:1, 1:2, and 2:1, based on the copolymer compositions estimated by quantitative ^{1}H NMR analysis. Before spin-coating, the silicon substrate was thoroughly washed with acetone, isopropyl alcohol, and toluene, while the PS substrate was washed with isopropyl alcohol. The polymer solution was spin-coated onto the desired substrate at 4000 rpm for 30 s, and UV light with a wavelength of 254 nm was illuminated with varying energy from 50 to 500 mJ/cm^2. For photopatterning, a photomask (18 μm line/18 μm space, 20 × 20 μm square with 25 μm space between squares) was placed on the thin film on the silicon or PS substrate, followed by exposure to UV light with optimized energy. All UV light-exposed samples were placed at room temperature for 10 min, followed by immersion in deionized (DI) water for 5 min and drying with a stream of Ar gas.

Post-Crosslinking Immobilization of BSA. A solution of MN and MD in ethanol (2.5 wt %, NBOC/DTC = 1:2) was spin-coated onto the washed PS substrate at 4000 rpm for 30 s, followed by photopatterning under UV light illumination at an intensity of 500 mJ/cm^2. Upon exposure, the sample was maintained at room temperature for 5 min, followed by development with DI water for 5 min. The sample was subjected to immersion in FITC-labeled BSA solution (FITC-BSA 5 mg in 9 mL of DI water and 1 mL of PBS) for 1 h. The sample was then washed by immersion in DI water for 1 min, followed by drying under a stream of Ar gas.

Photo-Crosslinking of Thin Films Consisting of fGelMA and Two Copolymers. MN and MG (NBOC/GMA = 1:1) and varied amounts of fGelMA from 10 to 100 wt % of MN/MG were dissolved in DI water to attain a concentration of the three polymer components of 2.5 wt %. For MN/MD, MN and MD (NBOC/DTC = 1:1) and various amounts of fGelMA from 10 to 100 wt % of MN/MD were dissolved in a certain amount of DI water, and ethanol was added to let the weight ratio of DI water and ethanol be 1:1.5 at a concentration of the three polymers of 2.5 wt %. To both, LAP was then added to the solution (5 wt % relative to the weight of fGelMA). Each homogeneous solution was spin-coated onto pre-cleaned silicon, glass, and PS substrates at 4000 rpm for 30 s. Then, the samples were exposed to UV light at a wavelength of 254 nm with an energy of 500 mJ/cm^2 with or without a mask. The samples were placed at room temperature for 10 min, immersed in DI water for 30 s, and dried under a stream of Ar gas. For FITC labeling, the thin film sample was dipped in an FITC solution (FITC 0.5 mg in 0.2 mL of DMSO and 10 mL of PBS) for 1 h, washed by immersion in water for 30 s, and dried with a stream of Ar gas.

Viability and Growth of C2C12 Myocytes on the Thin Film. To assess viability, C2C12 myocytes were seeded at a density of 10,000 cells/cm^2 on a thin film and cultured for 24 h at 37 °C/5% CO_2. Substrates were washed with PBS before a mixture of calcein-AM (2 μM, Biotum, cat# 30002A) and ethidium homodimer III (4 μM, Biotum, cat# 30002A) was added for 5 min at 37 °C/5% CO_2. Using a Nikon Ti2 inverted microscope equipped with a pco.edge 4.2 camera, all images were taken with a 20× objective lens (NA = 0.45) at an exposure time of 250 ms. The number of calcein-AM-positive cells divided by the total number of cells in each image was reported as the viability of each image. To assess the growth of C2C12 myocytes on each thin film, glass or PS substrates were taped to the bottom of a well in a 12-well plate using double-sided tape to prevent the surfaces from floating, followed by sterilization with 50 μg/mL gentamicin (Thermo Fisher, cat# 15750060) for 15 min. Next, C2C12 myocytes were seeded at a density of 10,000 cells/cm^2, cultured for 24 h at 37 °C/5% CO_2, fixed with 4% paraformaldehyde for 15 min, washed three times with PBS, permeabilized with 0.1% Triton-X 100 for 10 min, and washed three times with PBS again. To visualize cell attachment on the thin film, C2C12 myocytes were stained with phalloidin (10 μM, Biotium, cat# 00041), following the manufacturer's protocol, and counterstained with Hoechst 33342 (AnaSpec, cat# AS83218). Using the Nikon Ti2 inverted microscope equipped with a pco.edge 4.2 camera, all images were taken with a 20× objective lens (NA = 0.45) at an exposure time of 250 ms. Hoechst images were processed using FIJI software by automatically adjusting the image threshold with black and white settings, converting the image to a binary mask, and applying a binary watershed filter to separate adjacent cells. The number of cells was counted using the Analyze Particle program with size settings of 120 pixel^2−infinity, ignoring cells along the edge of the images. Phalloidin images were analyzed by automatically adjusting the brightness and contrast of the image and then automatically adjusting the threshold with black and white settings. Similar to the Hoechst 33342-stained images, phalloidin images were converted to a binary mask, with the total area and area fraction measured using FIJI software.

https://doi.org/10.1021/acs.chemmater.3c00225
Chem. Mater. XXXX, XXX, XXX−XXX

Table 1. Characteristics of Synthesized Copolymers

sample	M_n (kDa or kg/mol)[a]	$Đ$[a]	$F_{PEGMEMA}$[b]	F_{GMA}[b]	F_{DTCMMA}[b]	$F_{NBOCAEMA}$[b]
MG	19.7	1.26	0.794	0.206		
MD	15.3	1.38	0.840		0.160	
MN	16.5	1.27	0.826			0.174

[a]Determined with SEC. [b]Determined with quantitative ^{1}H NMR.

Scheme 2. Fabrication of the Photo-Crosslinked Thin Film and Micropatterns, and the Mechanism for the Crosslinking Reaction of the Photo-Released Primary Amine and DTC or Epoxy Units; PS, Polystyrene; GS, Glass

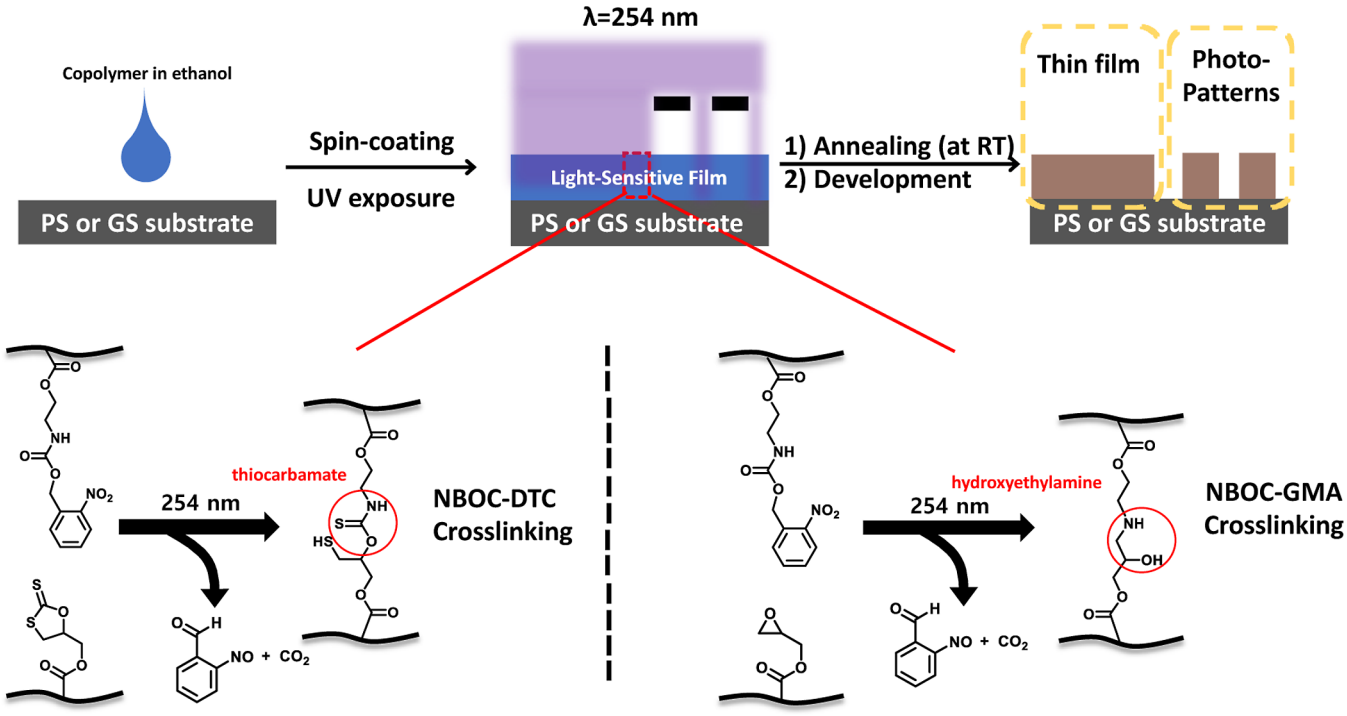

Characterization. ^{1}H NMR spectra were recorded on a JNM-ECZ400S 400 MHz spectrometer (JEOL) with the solvent of $CDCl_3$ or DMSO-d_6. Size exclusion chromatography (SEC) was performed using a Thermo Scientific Ultimate 3000 chromatography system to obtain molecular weight information. Chromatograms were recorded with an eluent of THF at 35 °C at a flow rate of 1 mL/min, followed by analysis with a calibration curve constructed using 10 standard PS samples (Shodex) in the M_n range of 1.22 to 2700 kg/mol. Optical microscopy images were obtained using an Olympus BX53M optical microscope. Confocal laser scanning microscopy (CLSM; LSM 510 META) was used to observe the fluorescence from a surface labeled with FITC at an excitation wavelength of 488 nm. The thin film thickness was measured using a spectroscopic ellipsometer (SE MG-1000, Nano-View Co. Ltd.) in the detection wavelength range of 350−840 nm. X-ray photoelectron spectroscopy (XPS, K-Alpha, Thermo Scientific) was employed to analyze the chemical composition of the thin film surface.

RESULTS AND DISCUSSION

Synthesis of Reactive PEGMEMA-Containing Random Copolymers. Three types of copolymers—poly(PEGMEMA-*r*-NBOCAEMA) (MN), poly(PEGMEMA-*r*-GMA) (MG), and poly(PEGMEMA-*r*-DTCMMA) (MD)—were synthesized by RAFT copolymerization (Scheme 1). In all cases, most components are PEGMEMA, which allows good solubility of the copolymers in various polar solvents, including water and alcohols, ensuring that the copolymers can be coated on a variety of inorganic and organic substrates. Two types of functionalities were considered the second monomer: (i) the NBOC group in NBOCAEMA releasing the nucleophilic primary amine upon UV light illumination and (ii) the reactive epoxy group in GMA or the cyclic dithiocarbonate group in DTCMMA, which is expected to readily undergo a ring-opening reaction with the primary amine. The feed ratios of PEGMEMA and the second monomer (NBOCAEMA, GMA, or DTCMMA) were set to 0.800 and 0.200, respectively. As tabulated in Table 1, the molecular weight (M_n) of the copolymers was achieved between 10 and 20 kDa (or kg/mol), with its distribution in the SEC measurement found to be unimodal with the dispersity ($Đ$) less than 1.4 (Figure S1), suggesting that the RAFT copolymerization of three different monomer pairs was effectively regulated. $F_{PEGMEMA}$ of the copolymers, characterized by quantitative ^{1}H NMR (Figure S1), varied from 0.79 to 0.84, which did not significantly deviate from the feed ratio; hence, the concentrations of reactive groups in MN, MG, and MD are expected to be sufficient for effective crosslinking between MN and MG or between MN and MD.

Binary Copolymer Systems for Photo-Crosslinking and Photopatterning in Thin Films. To achieve effective crosslinking, thin film systems were designed by combining two types of copolymers: (i) MN with photocleavable NBOC groups and (ii) MG or MD bearing electrophilic ring moieties, i.e., MN/MG and MN/MD mixed binary component systems. The *o*-nitrobenzyl group in MN is cleaved to release the

https://doi.org/10.1021/acs.chemmater.3c00225
Chem. Mater. XXXX, XXX, XXX−XXX

primary amine group upon exposure to UV light (λ = 254 nm).[40,41] In the binary system, the dithiocarbonate ring or glycidyl groups are attacked by the released nucleophilic primary amine to form thiocarbamate or hydroxyethylamine bonds, resulting in interchain photo-crosslinking (Scheme 2). In addition, the crosslinking reaction between the primary amine and reactive rings can be facilitated due to the enhanced chain mobility as PEG-based materials typically exhibit a T_g lower than room temperature.[42−44] It has been known that at the temperature higher than T_g, the chain mobility increases, and therefore, the possibility of a certain reaction also can be increased.[45−47] Therefore, the crosslinking reaction is readily accomplished even at room temperature, enabling substrate independence; in other words, organic-based materials, which can easily deform by heating to induce crosslinking, can be utilized as a substrate. Moreover, using UV light enabled transferring the image in a photomask to the thin film of the copolymer mixture.

The compositions of MN/MD and MN/MG were varied to control their surface chemical properties. Copolymer solutions for spin-coating were prepared by systematically varying the molar ratio of GMA (or DTC) and NBOC monomers in the MG (or MD) and MN, i.e., 1:1, 1:2, and 2:1. Using this approach, unreacted functional groups remained after photo-crosslinking. For example, a thin film made from MN/MD (1:2 or 2:1) is expected to bear an unreacted DTC ring or primary amine on its surface after crosslinking. The unreacted reactive functionalities is possibly subjected to subsequent reactions to molecularly define the desired reactive functionality on the coating. MN/MG and MN/MD with varied compositions were assessed as a function of UV light energy (Figure 1) by measuring the film thickness after exposure to the desired energy and subsequent development with DI water. All systems showed similar results: the crosslinking reaction began at ≈100 mJ/cm^2 and was completed at ≈300 mJ/cm^2 without post-exposure heating. The chemical compositions of the thin films were further examined using XPS. Before illumination with UV light, the peak at ≈405 eV, assigned to N 1s of NO_2,[29] was observed in both MN/MG and MN/MD thin films (Figure S2). The peak disappeared completely after UV illumination (Figure S2), indicating that the cleavage reaction of the *o*-nitrobenzyl group occurred. In addition, typically, nitrogen from NO can be found at ≈401 eV;[48] however, only one peak at 398−400 eV was observed, strongly suggesting that the byproduct, *o*-nitrosobenzaldehyde, was fully removed during the post-crosslinking immersion process. The crosslinking and change in the chemical composition of the thin films confirm that the binary component systems are effective in attaining the desired properties. Figure S3 shows the negative tone line/space (half pitch = 18 μm) and square (side = 20 μm) photopatterns in the six types of thin films fabricated with an illumination energy of 500 mJ/cm^2 and developed in DI water for 5 min, further confirming that photo-crosslinking is effectively controlled even for successful photoimaging.

To examine the compatibility of the copolymers with different substrates, i.e., substrate independence, both MN/MG and MN/MD (1:1) solutions were prepared and coated on various substrates, including silicon, glass, plastics, and metals. The water contact angle measurements of the MN/MG and MN/MD thin films fabricated on various substrates are shown in Figure 2, and representative water contact angle measurements are shown in Figure S4. Before depositing the

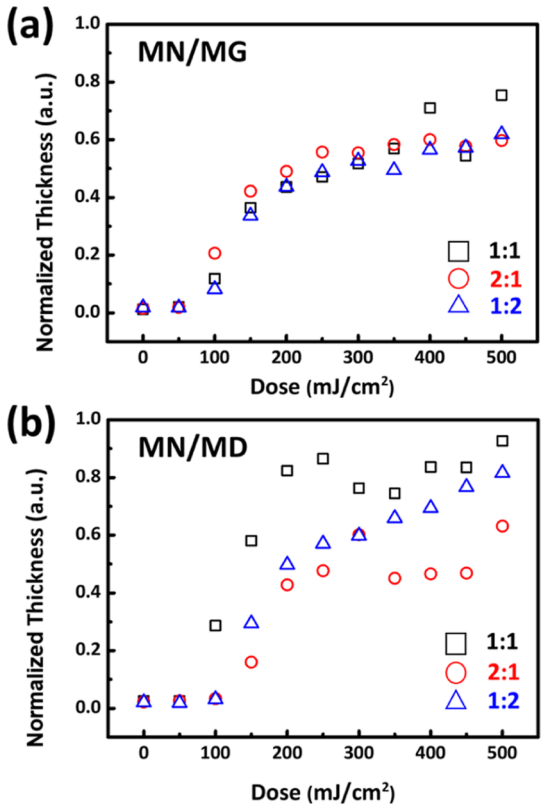

Figure 1. Film thickness (normalized to film thickness before crosslinking) as a function of the energy of illuminating UV light for (a) MN/MG and (b) MN/MD systems. The molar ratios of NBOC to epoxy or DTC unit were set to 2:1, 1:1, and 1:2 for both MN/MG and MN/MD systems.

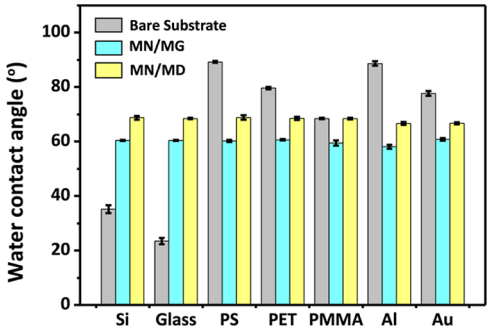

Figure 2. Water contact angle measurements of different substrates before and after deposition of MN/MG and MN/MD thin films.

thin films, the water contact angle was varied depending on the substrate; however, the water contact angles of all samples coated with MN/MG and MN/MD thin films were similar with the average values of 60.01° ± 0.95° and 68.20° ± 0.78°, respectively. These results strongly suggest that the binary copolymer system was successfully deposited on many types of the substrates.

Post-Crosslinking Functionalization with the Remaining Surface Reactive Group. The photo-crosslinked thin films were subjected to post-crosslinking functionalization. Controlling the surface functionality of the crosslinked pattern may lead to the formation of more complex and diverse surfaces for designated applications. As a proof of concept, we investigated the immobilization of BSA onto the surface of the

https://doi.org/10.1021/acs.chemmater.3c00225
Chem. Mater. XXXX, XXX, XXX−XXX

Scheme 3. Surface Functionalization with FITC-Labelled BSA

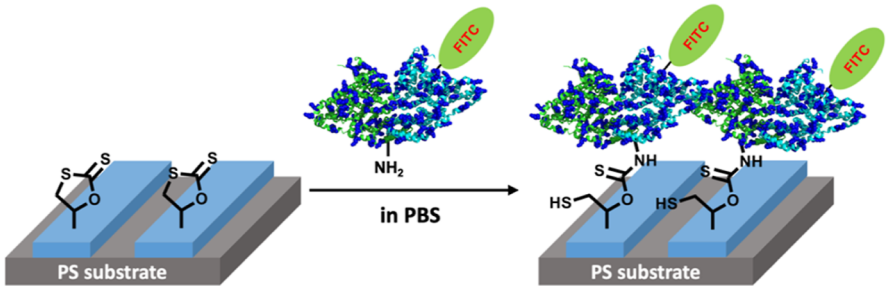

photopatterned patches. Dual-component systems can yield two types of reactive groups—primary amines and reactive DTC rings—by controlling the composition of the components. As BSA is known to have 60 lysine residues, of which approximately more than 50% of the primary amine can act as a nucleophile for bioconjugation or coupling of peptides,[49,50] the composition of MN/MD was controlled to 1:2 to ensure that intact DTC units, which react with the primary amine in BSA, are available on the surface of the crosslinked region (Scheme 3). The immobilization process was conducted by simple immersion of the thin film samples on a silicon wafer and PS substrate into a solution of FITC-labeled BSA in PBS at room temperature. The immobilized BSA can be readily identified by fluorescence microscopy. Figure 3a shows a

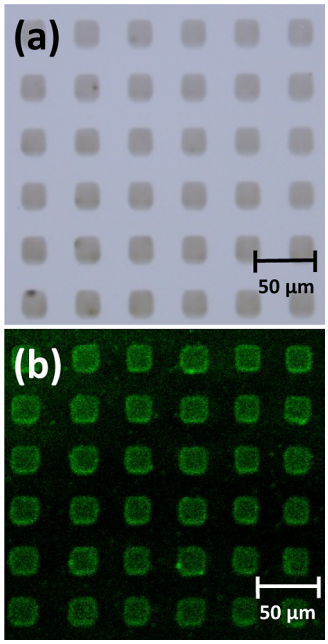

Figure 3. (a) Micrographs of photopatterned MN/MD on the silicon substrate and (b) fluorescence micrographs of the MN/MD photopatterns on the PS substrate after surface functionalization with FITC-labeled BSA.

successfully fabricated photopattern with MN/MD (1:2) on a silicon wafer. The same pattern was formed on the PS substrate, subsequently subjected to post-crosslinking immobilization of BSA under the same conditions. As shown in Figure 3b, the fluorescent domains were defined on the square patterns on the PS, confirming the designed chemical route to immobilize the target molecules onto the selective region. Furthermore, controlling the composition of the thin film is effective for incorporating the desired surface reactive groups and attaining the desired surface (bio)chemical properties.

Photo-Induced Fabrication of Composite Thin Films Conferring Surface Activity. The application of crosslinkable systems was further explored to create surfaces that can be used to regulate the proliferation or differentiation of mammalian cells. Therefore, we designed composite thin films by simply mixing MN/MG or MN/MD with a third component that can exhibit surface activity. fGel was selected because of its straightforward anchoring points for cell attachment, its chemical versatility to incorporate reactive groups, and its abundance and sustainability.[36,51−54] However, the primary amine of lysine in the fGel can react with DTC or glycidyl groups, making it challenging to prepare the composite thin film from the coating solution. To overcome this issue, we modified fGel to incorporate methacrylate units, which can act as crosslinkable units in the presence of a radical species, by reacting the primary amine with the glycidyl group in glycidyl methacrylate, i.e., fGelMA.[35,36,39] In this design, two crosslinking mechanisms are considered after UV light illumination: (i) addition of the released primary amine from NBOC in MN with DTC or glycidyl groups in the MD or MG chain and (ii) a radical-based reaction of the methacrylate in fGelMA (Scheme 4) with the use of a photo-radical generator (LAP). In the case of the MN/MG system, the vinyl groups in the fGelMA chains were bonded to each other to form interchain bridges upon exposure, with the resulting fGelMA network expected to be intertwined and physically interact with another network formed by interchain reactions between the MN and MG chains. The MN/MD system also has a similar structure, and it is expected that the vinyl group in fGelMA reacts with the thiol group released by the ring-opening reaction of DTC with the amine from NBOC through a radical-based thiol-ene click reaction. As two types of crosslinkings can occur, several crosslinking points are expected to form, leading to a stable composite thin film.

Through a series of formulation tests, solutions of MN/MG/fGelMA/LAP or MN/MD/fGelMA/LAP with varying amounts of fGelMA [the extent of the addition reaction of the primary amine in fGel for methacrylate (DA) = 0.920; 10−100 wt % relative to the mass of MN and MG (or MD) copolymers] were prepared with DI water or 60 wt % ethanol solution in DI water as a solvent. Spin-coating of the solutions prepared with other types of solvents resulted in the formation of non-uniform thin films. All spin-coated films were exposed to 254 nm UV light with an energy density of 500 mJ/cm^2, followed by development with DI water. The resulting pattern on silicon was observed with bright field microscopy, and the pattern on PS was labeled with FITC and examined by using CLSM, as shown in Figure 4, confirming that the material

https://doi.org/10.1021/acs.chemmater.3c00225
Chem. Mater. XXXX, XXX, XXX−XXX

Scheme 4. Schemes of Dual Photo-Crosslinking in Composite Thin Films of MN/MG/fGelMA and MN/MD/fGelMA

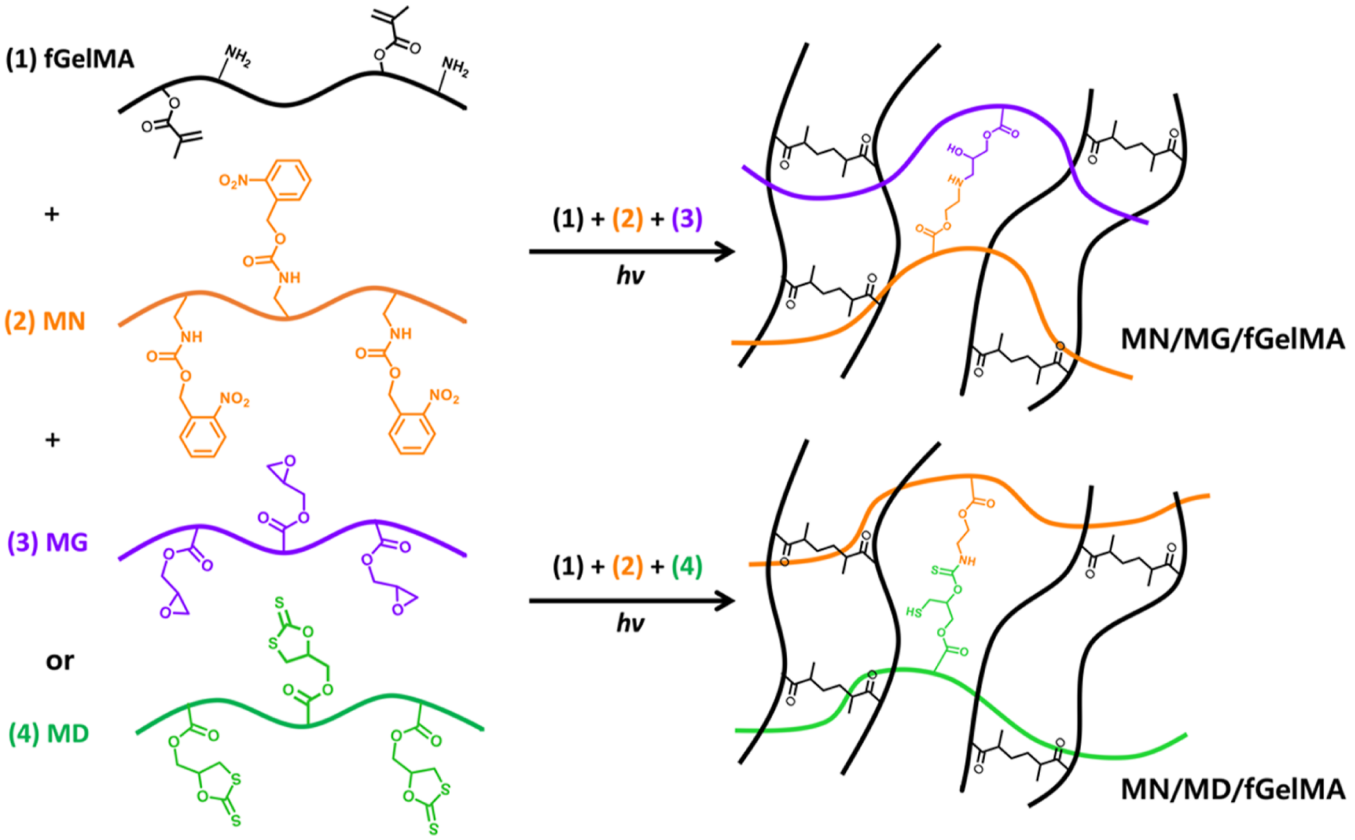

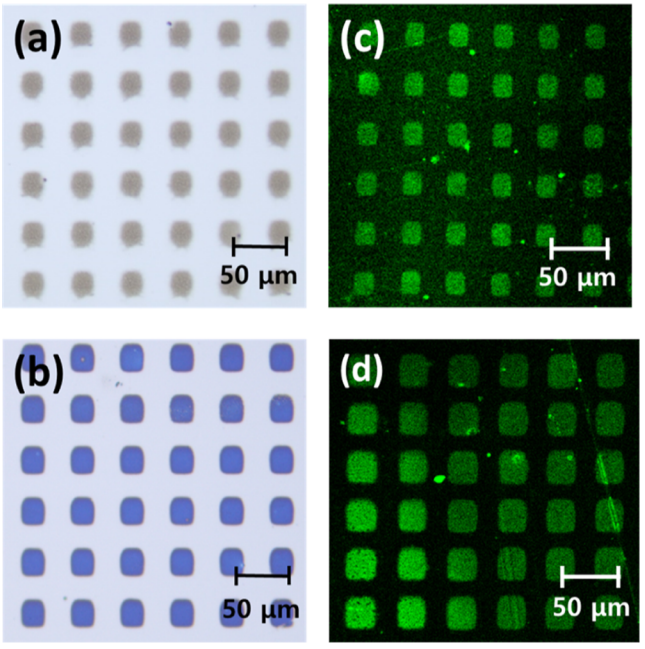

Figure 4. Bright field (a,b) and fluorescence micrographs (c,d) showing photopatterns of (a,c) MN/MG with 50 wt % fGelMA thin films and (b,d) MN/MD with 50 wt % fGelMA thin films. Substrates used in bright field and fluorescence microscopy are silicon and PS, respectively.

design is highly effective in forming photo-crosslinked organic composite coatings without heating. Notably, the amount of fGelMA, i.e., the bioactive domain that confers surface activity, can be tuned in thin films. The thickness of both the MN/MG and MN/MD thin films increased with an increase in the amount of incorporated fGelMA (Table S1). The chemical composition of the thin films of MN/MG and MN/MD systems with a systematic variation in the quantity of incorporated fGelMA was examined by CLSM and XPS. Figure S5a,b shows the fluorescence micrographs of thin films fabricated with both systems by varying the amount of fGelMA incorporated. The thin films were labeled with FITC conjugated to the remaining amine in the fGelMA. All the thin films emitted a positive green fluorescence signal, and the trend of a gradual increase in mean fluorescence intensity was observed as the concentration of fGelMA increased (Figure S5c). In the XPS spectra (Figure S6), the relative intensity of the N 1s peak at ≈400 eV tended to increase with increasing incorporation of fGelMA. Consequently, an increase in the atomic percentage of *N* was observed (Table 2), confirming that the concentration of a specific component can be effectively varied in the stable coating.

We further examined the role of the fGelMA methacrylate in the crosslinking reaction. The DA was controlled by varying the reaction conditions between 0.143 and 0.920 (Figure S7). MN/MG and MN/MD thin films were deposited at two different degrees of the addition, with their thicknesses measured before and after the crosslinking process (Table S2). Both thin films with fGelMA with a DA of 0.143 were almost completely dissolved by post-exposure immersion in DI water, while the systems with fGelMA with a DA of 0.920 were effectively crosslinked. Figure S8 shows the photopatterns of MN/MG with fGelMA (DA = 0.143) at various times for the post-exposure immersion process. The photopattern was observed when the sample was immersed for a short period

https://doi.org/10.1021/acs.chemmater.3c00225
Chem. Mater. XXXX, XXX, XXX−XXX

Table 2. Compositions of Characteristic Elements in Photo-Crosslinked Composite Thin Films Characterized Using XPS

sample	element	fGelMA 10 wt %	fGelMA 50 wt %	fGelMA 100 wt %
MN/MG	N	0.8%	1.1%	1.3%
	O	24.8%	25.6%	25.5%
	C	74.3%	73.3%	73.2%
MN/MD	N	1.0%	1.2%	1.8%
	O	24.5%	24.3%	24.7%
	S	0.8%	0.8%	0.6%
	C	73.8%	73.7%	72.8%

of time (30 s), suggesting that the system was crosslinked. However, immersion for a longer time led to pattern damage, strongly suggesting that the crosslinking density was not high enough to produce a fully stable pattern. However, fGelMA with a high DA was highly effective in producing stable photopatterns (Figures S8–S10). This observation confirms that the radical-based crosslinking mechanism is equally important; hence, an effective dual crosslinking system was established with the current material design.

Cell Viability and Growth Area on the Composite Thin Films. The viability of C2C12 myocytes on thin films was not altered by varying the amount of fGelMA (Figure 5a,b). However, we observed a slight but non-significant

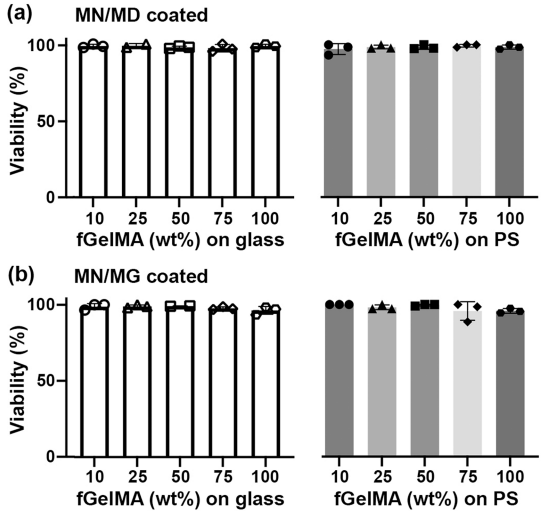

Figure 5. Viability of C2C12 myocytes cultured on thin films of MN/MD (a) and MN/MG (b) with the increasing fractions of fGelMA on glass and PS. Mean ± SD, $n = 3$, no significant difference after one way ANOVA and Tukey's *post hoc* tests ($\alpha = 0.05$).

decrease in C2C12 myocyte viability on thin films containing MN/MG and higher concentrations of fGelMA (Figure 5b). Thus, photopatterning chemistry did not inhibit the initial attachment of C2C12 myocytes, regardless of the thin film precursors of photo-crosslinking and the concentration of fGelMA.

As shown in Figure 6, the area occupied by each C2C12 myocyte was not significantly different on thin films with respect to the thin film precursors of photo-crosslinking or the concentration of fGelMA. The normalized growth area per cell was more consistent with MN/MG (Figure 6c,d) than with MN/MD (Figure 6a,b). While both normalized growth area and viability are hardly distinguished by the photopatterning chemistry or the incorporated quantity of fGelMA, the number of cells attached exhibited high (Pearson's $r = 0.752$, MN/MD on PS) to very high (Pearson's $r = 0.913$, MN/MD on glass; Pearson's $r = 0.857$, MN/MG on glass; and Pearson's $r = 0.892$, MN/MG on PS) correlation, as evidenced in Figures 6b,d and S11. Tissue culture surfaces are commonly treated with oxygen plasma to increase hydrophilicity;[55] however, this process is far less functional than any direct functionalization or conjugation. Multiple methods have successful and reproducible functionalization of tissue culture surfaces with poly-lysine or poly-ethylimine, poly-L-ornithine, gelatin, and ECM proteins at concentrations less than 1 mg/mL by modulating the charges on tissue culture surfaces.[56−58] While these non-specific coatings still facilitate cell attachment and growth of many different cell types, this may cause significant interference or uncontrolled differentiation and proliferation of human pluripotent stem cells. Klim et al. showed that surfaces decorated with the glycosaminoglycan-binding domain derived from vitronectin support the self-renewal of multiple pluripotent stem cell lines over 3 months.[59] For cardiomyocyte differentiation, only laminin-derived matrices support long-term adhesion (over 15 days) using the chemically defined medium including Roswell Park Memorial Institute 1640 basal medium, L-ascorbic acid 2-phosphate, and BSA.[60] Therefore, the potential of the proposed straightforward modification of culture surfaces with ECM proteins[61] is to avoid or significantly reduce the time for assay optimization with too many unknown variables.

CONCLUSIONS

In summary, we demonstrated a polymer thin film capable of simultaneously overcoming various challenges associated with methodologies for achieving organic coating systems that simultaneously address the current challenges in surface engineering: (i) processability on both organic and inorganic substrates; (ii) versatility and adjustability for defining specific active surface chemical functionalities with post-crosslinking modifications or incorporation of the third functional component for composite systems; (iii) patternable, clean, and scalable systems that can be attained through easy fabrication processes; and (iv) applicability in a certain field, i.e., interfacing biological objects. As organic solvents used in general surface processing damage polymer substrates, a polymer precursor was synthesized to show that it can be dissolved in polar solvents, such as water and alcohol, without causing any detrimental effects on the polymer substrate. The polymers consist of a PEG-based methacrylate soluble in polar solvents, NBOCAEMA which forms a reactive functional group by deprotection by UV irradiation, and GMA and DTCMMA having a reactive functional group that can easily react under mild conditions. The thin film made of the synthesized polymer could easily form a thin film on various substrates such as glass, silicon, plastics, and metals and was easily crosslinked at room temperature by UV irradiation. It was also possible to prepare a stable thin film by mixing fGelMA to ensure that the cells could attach and grow on the surface. In addition, it was shown that a stable thin film was formed by mixing a polar synthetic polymer with a complex natural polymer. The current design is highly beneficial as it is a simple, clean, and chemically adjustable system readily achievable under mild processing conditions. Copolymer design also enabled tailoring the surface functionalities by

https://doi.org/10.1021/acs.chemmater.3c00225
Chem. Mater. XXXX, XXX, XXX−XXX

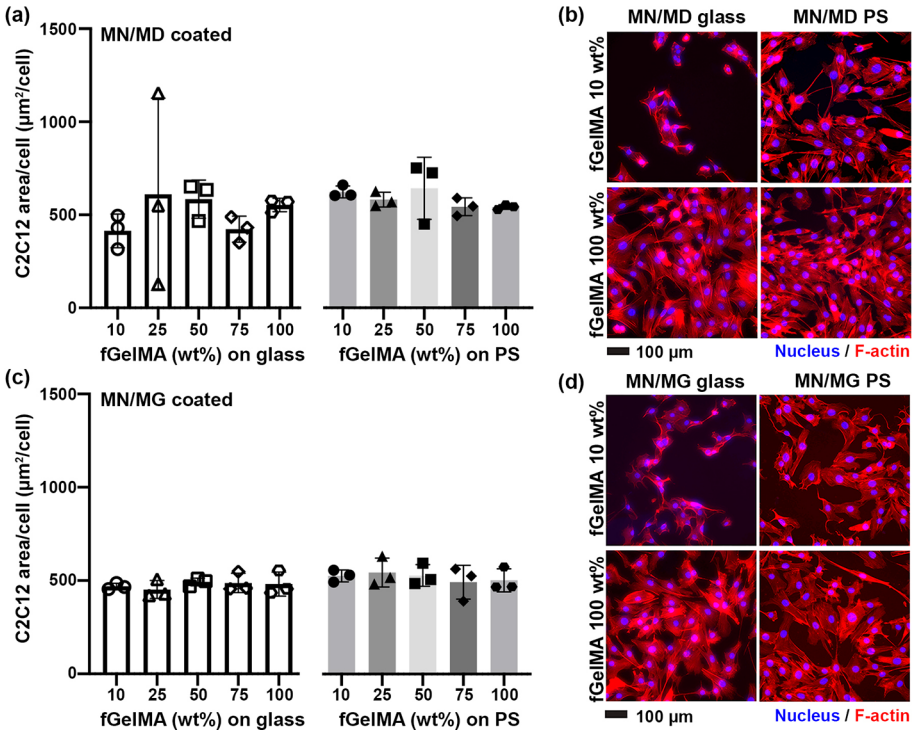

Figure 6. Normalized growth area of C2C12 myocytes cultured on thin films of MN/MD (a) and MN/MG (c) with the increasing fractions of fGelMA on glass and PS, and corresponding representative images (b,d). Mean ± SD, n = 3, no significant difference after one way ANOVA and Tukey's *post hoc* tests (α = 0.05).

tuning the comonomer structure and composition. For engineered features, all the materials could form patterns through photolithography, and the surface biocompatibility implies further utility in highly regulated culture microenvironments or cell−matrix interactions.

■ ASSOCIATED CONTENT

Supporting Information

The Supporting Information is available free of charge at https://pubs.acs.org/doi/10.1021/acs.chemmater.3c00225.

^{1}H NMR spectra and SEC chromatograms; XPS spectra; optical microscopy images of fabricated patterns; images showing water contact angle measurement; thicknesses of the composite thin films; fluorescence micrographs of fluorophore-labeled thin films; and fluorescence micrographs showing C2C12 myocytes on the thin films (PDF)

■ AUTHOR INFORMATION

Corresponding Authors

Jangwook P. Jung − *Department of Biological Engineering, Louisiana State University, Baton Rouge, Louisiana 70803, United States;* orcid.org/0000-0001-5783-4549; Email: jjung1@lsu.edu

Myungwoong Kim − *Department of Chemistry and Chemical Engineering, Inha University, Incheon 22212, Republic of Korea;* orcid.org/0000-0003-0611-8694; Email: mkim233@inha.ac.kr

Authors

Seungyeon Choi − *Department of Chemistry and Chemical Engineering, Inha University, Incheon 22212, Republic of Korea*

Lane D. Yutzy − *Department of Biological Engineering, Louisiana State University, Baton Rouge, Louisiana 70803, United States*

Yun Hee Ko − *Department of Chemistry and Chemical Engineering, Inha University, Incheon 22212, Republic of Korea*

Jin-Kyun Lee − *Program in Environment and Polymer Engineering and Department of Polymer Science and Engineering, Inha University, Incheon 22212, Republic of Korea;* orcid.org/0000-0001-9468-5749

Complete contact information is available at: https://pubs.acs.org/10.1021/acs.chemmater.3c00225

Author Contributions

S.C. and L.D.Y. contributed equally. The manuscript was written based on contributions from all authors. All authors have given approval to the final version of the manuscript.

Notes

The authors declare no competing financial interest.

■ ACKNOWLEDGMENTS

We acknowledge support from the Korea Evaluation Institute of Industrial Technology (KEIT) funded by the Ministry of Trade, Industry and Energy (MOTIE) of the Republic of Korea (project no. 20012622), the National Research Foundation of Korea funded by the Ministry of Science and ICT (MSIT) of the Republic of Korea (grant no. 2021R1A2C1093999), the National Science Foundation CAREER Award (DMR 2047018, J.P.J.), the LSU Faculty Research Grant—Emerging Research (J.P.J.), and the Donald W. Clayton Scholarship from the LSU College of Engineering (L.D.Y.). S.C. and Y.H.K. acknowledge the partial support by the Korea Institute for Advancement of Technology (KIAT)

grant funded by the Korea Government (MOTIE) (P0008458, The Competency Development Program for Industry Specialist).

REFERENCES

(1) Schmitt, S. K.; Trebatoski, D. J.; Krutty, J. D.; Xie, A. W.; Rollins, B.; Murphy, W. L.; Gopalan, P. Peptide Conjugation to a Polymer Coating Via Native Chemical Ligation of Azlactones for Cell Culture. *Biomacromolecules* **2016**, *17*, 1040−1047.
(2) Chen, X.; Sevilla, P.; Aparicio, C. Surface Biofunctionalization by Covalent Co-Immobilization of Oligopeptides. *Colloids Surf., B* **2013**, *107*, 189−197.
(3) Mrksich, M.; Whitesides, G. M. Using Self-Assembled Monolayers to Understand the Interactions of Man-Made Surfaces with Proteins and Cells. *Annu. Rev. Biophys. Biomol. Struct.* **1996**, *25*, 55−78.
(4) Slaughter, B. V.; Khurshid, S. S.; Fisher, O. Z.; Khademhosseini, A.; Peppas, N. A. Hydrogels in Regenerative Medicine. *Adv. Mater.* **2009**, *21*, 3307−3329.
(5) Xue, Y.; Liu, D.; Wang, C.; Bao, C.; Wang, X.; Zhu, H.; Mao, H.; Cai, Z.; Lin, Q.; Zhu, L. Photo and Reduction Dual-Responsive Hydrogel for Regulating Cell Adhesion and Cell Sheet Harvest. *ACS Appl. Bio Mater.* **2020**, *3*, 2410−2418.
(6) Shimizu, T.; Yamato, M.; Kikuchi, A.; Okano, T. Two-Dimensional Manipulation of Cardiac Myocyte Sheets Utilizing Temperature-Responsive Culture Dishes Augments the Pulsatile Amplitude. *Tissue Eng.* **2001**, *7*, 141−151.
(7) Ito, Y. Surface Micropatterning to Regulate Cell Functions. *Biomaterials* **1999**, *20*, 2333−2342.
(8) Liu, H.; Ito, Y. Gradient Micropattern Immobilization of a Thermo-Responsive Polymer to Investigate Its Effect on Cell Behavior. *J. Biomed. Mater. Res., Part A* **2003**, *67A*, 1424−1429.
(9) Wu, B.; Kumar, A. Extreme Ultraviolet Lithography and Three Dimensional Integrated Circuit-a Review. *Appl. Phys. Rev.* **2014**, *1*, 011104.
(10) Edwards, E. W.; Montague, M. F.; Solak, H. H.; Hawker, C. J.; Nealey, P. F. Precise Control over Molecular Dimensions of Block-Copolymer Domains Using the Interfacial Energy of Chemically Nanopatterned Substrates. *Adv. Mater.* **2004**, *16*, 1315−1319.
(11) Zhang, L.; Lin, J.; Lin, S. Self-Assembly Behavior of Amphiphilic Block Copolymer/Nanoparticle Mixture in Dilute Solution Studied by Self-Consistent-Field Theory/Density Functional Theory. *Macromolecules* **2007**, *40*, 5582−5592.
(12) Trombly, D. M.; Pryamitsyn, V.; Ganesan, V. Surface Energies and Self-Assembly of Block Copolymers on Grafted Surfaces. *Phys. Rev. Lett.* **2011**, *107*, 148304.
(13) Rundqvist, J.; Hoh, J. H.; Haviland, D. B. Directed Immobilization of Protein-Coated Nanospheres to Nanometer-Scale Patterns Fabricated by Electron Beam Lithography of Poly(ethylene glycol) Self-Assembled Monolayers. *Langmuir* **2006**, *22*, 5100−5107.
(14) Albert, J. N. L.; Epps, T. H., III. Self-Assembly of Block Copolymer Thin Films. *Mater. Today* **2010**, *13*, 24−33.
(15) Onses, M. S.; Ramírez-Hernández, A.; Hur, S.-M.; Sutanto, E.; Williamson, L.; Alleyne, A. G.; Nealey, P. F.; de Pablo, J. J.; Rogers, J. A. Block Copolymer Assembly on Nanoscale Patterns of Polymer Brushes Formed by Electrohydrodynamic Jet Printing. *ACS Nano* **2014**, *8*, 6606−6613.
(16) Hamley, I. W. Ordering in Thin Films of Block Copolymers: Fundamentals to Potential Applications. *Prog. Polym. Sci.* **2009**, *34*, 1161−1210.
(17) Popat, K. C.; Mor, G.; Grimes, C. A.; Desai, T. A. Surface Modification of Nanoporous Alumina Surfaces with Poly(ethylene glycol). *Langmuir* **2004**, *20*, 8035−8041.
(18) Thiry, D.; Pouyanne, M.; Cossement, D.; Hemberg, A.; Snyders, R. Surface Engineering of Bromine-Based Plasma Polymer Films: A Step toward High Thiol Density Containing Organic Coatings. *Langmuir* **2018**, *34*, 7655−7662.
(19) Sartori, S.; Rechichi, A.; Vozzi, G.; D'Acunto, M.; Heine, E.; Giusti, P.; Ciardelli, G. Surface Modification of a Synthetic Polyurethane by Plasma Glow Discharge: Preparation and Characterization of Bioactive Monolayers. *React. Funct. Polym.* **2008**, *68*, 809−821.
(20) Garg, S.; Hurren, C.; Kaynak, A. Improvement of Adhesion of Conductive Polypyrrole Coating on Wool and Polyester Fabrics Using Atmospheric Plasma Treatment. *Synth. Met.* **2007**, *157*, 41−47.
(21) Konno, T.; Hasuda, H.; Ishihara, K.; Ito, Y. Photo-Immobilization of a Phospholipid Polymer for Surface Modification. *Biomaterials* **2005**, *26*, 1381−1388.
(22) Yang, W.-C.; Wu, S.-H.; Chen, Y.-F.; Nelson, A.; Wu, C.-M.; Sun, Y.-S. Effects of the Density of Chemical Cross-Links and Physical Entanglements of Ultraviolet-Irradiated Polystyrene Chains on Domain Orientation and Spatial Order of Polystyrene-*block*-Poly(methyl methacrylate) Nano-Domains. *Langmuir* **2019**, *35*, 14017−14030.
(23) Falconnet, D.; Koenig, A.; Assi, F.; Textor, M. A Combined Photolithographic and Molecular-Assembly Approach to Produce Functional Micropatterns for Applications in the Biosciences. *Adv. Funct. Mater.* **2004**, *14*, 749−756.
(24) Wang, R.; Chen, W.; Meng, F.; Cheng, R.; Deng, C.; Feijen, J.; Zhong, Z. Unprecedented Access to Functional Biodegradable Polymers and Coatings. *Macromolecules* **2011**, *44*, 6009−6016.
(25) Ito, Y.; Hasuda, H.; Sakuragi, M.; Tsuzuki, S. Surface Modification of Plastic, Glass and Titanium by Photoimmobilization of Polyethylene Glycol for Antibiofouling. *Acta Biomater.* **2007**, *3*, 1024−1032.
(26) Sason, E.; Kolitz-Domb, M.; Chill, J. H.; Margel, S. Engineering of Durable Antifog Thin Coatings on Plastic Films by UV-Curing of Proteinoid Prepolymers with PEG-Diacrylate Monomers. *ACS Omega* **2019**, *4*, 9352−9360.
(27) Schmitt, S. K.; Xie, A. W.; Ghassemi, R. M.; Trebatoski, D. J.; Murphy, W. L.; Gopalan, P. Polyethylene Glycol Coatings on Plastic Substrates for Chemically Defined Stem Cell Culture. *Adv. Healthcare Mater.* **2015**, *4*, 1555−1564.
(28) Liu, Q.; Xu, N.; Fan, L.; Ding, A.; Dong, Q. Polyacrylonitrile (PAN)/TiO_2 Mixed Matrix Membrane Synthesis by Thermally Induced Self-Crosslinking for Thermal and Organic-Solvent Resistant Filtration. *Chem. Eng. Sci.* **2020**, *228*, 115993.
(29) Lee, D. J.; An, S.; Nam, J.; Park, G.; Kim, S.; Kim, M. Light-Mediated Formation of Reactive Surface Chemical Patterns Using Thermally Crosslinkable Photosensitive Copolymers. *Bull. Korean Chem. Soc.* **2020**, *41*, 675−681.
(30) Kim, G.; An, S.; Hyeong, S.-K.; Lee, S.-K.; Kim, M.; Shin, N. Perovskite Pattern Formation by Chemical Vapor Deposition Using Photolithographically Defined Templates. *Chem. Mater.* **2019**, *31*, 8212−8221.
(31) Wang, X.; Liu, G.; Hu, J.; Zhang, G.; Liu, S. Concurrent Block Copolymer Polymersome Stabilization and Bilayer Permeabilization by Stimuli-Regulated "Traceless" Crosslinking. *Angew. Chem., Int. Ed.* **2014**, *53*, 3138−3142.
(32) Zhao, H.; Theato, P. Copolymers Featuring Pentafluorophenyl Ester and Photolabile Amine Units: Synthesis and Application as Reactive Photopatterns. *Polym. Chem.* **2013**, *4*, 891−894.
(33) Le Luyer, S.; Guégan, P.; Illy, N. Episulfide Anionic Ring-Opening Polymerization Initiated by Alcohols and Primary Amines in the Presence of γ-Thiolactones. *Macromolecules* **2022**, *55*, 5430−5440.
(34) Acocella, M. R.; Corcione, C. E.; Giuri, A.; Maggio, M.; Maffezzoli, A.; Guerra, G. Graphene Oxide as a Catalyst for Ring Opening Reactions in Amine Crosslinking of Epoxy Resins. *RSC Adv.* **2016**, *6*, 23858−23865.
(35) Son, D.; Hwang, H.; Fontenot, J. F.; Lee, C.; Jung, J. P.; Kim, M. Tailoring Physical Properties of Dual Network Acrylamide Hydrogel Composites by Engineering Molecular Structures of the Crosslinked Network. *ACS Omega* **2022**, *7*, 30028−30039.
(36) Belgodere, J.; Son, D.; Jeon, B.; Choe, J.; Guidry, A.; Bao, A.; Zamin, S.; Parikh, U.; Balaji, S.; Kim, M.; Jung, J. Attenuating Fibrotic

https://doi.org/10.1021/acs.chemmater.3c00225
Chem. Mater. XXXX, XXX, XXX−XXX

Markers of Patient-Derived Dermal Fibroblasts by Thiolated Lignin Composites. *ACS Biomater. Sci. Eng.* **2021**, *7*, 2212−2218.
(37) Kihara, N.; Nakawaki, Y.; Endo, T. Preparation of 1,3-Oxathiolane-2-Thiones by the Reaction of Oxirane and Carbon Disulfide. *J. Org. Chem.* **1995**, *60*, 473−475.
(38) Moad, G.; Chong, Y. K.; Postma, A.; Rizzardo, E.; Thang, S. H. Advances in RAFT Polymerization: The Synthesis of Polymers with Defined End-Groups. *Polymer* **2005**, *46*, 8458−8468.
(39) Wang, Z.; Tian, Z.; Menard, F.; Kim, K. Comparative Study of Gelatin Methacrylate Hydrogels from Different Sources for Biofabrication Applications. *Biofabrication* **2017**, *9*, 044101.
(40) Bochet, C. G. Photolabile Protecting Groups and Linkers. *J. Chem. Soc., Perkin Trans. 1* **2002**, 125−142.
(41) Piloto, A. M.; Costa, S. P. G.; Gonçalves, M. S. T. Wavelength-Selective Cleavage of *o*-Nitrobenzyl and Polyheteroaromatic Benzyl Protecting Groups. *Tetrahedron* **2014**, *70*, 650−657.
(42) Choi, I.; Kang, S. K.; Lee, J.; Kim, Y.; Yi, J. In situ Observation of Biomolecules Patterned on a PEG-Modified Si Surface by Scanning Probe :Ithography. *Biomaterials* **2006**, *27*, 4655−4660.
(43) Xu, H.; Kaar, J. L.; Russell, A. J.; Wagner, W. R. Characterizing the Modification of Surface Proteins with Poly(ethylene glycol) to Interrupt Platelet Adhesion. *Biomaterials* **2006**, *27*, 3125−3135.
(44) Groll, J.; Haubensak, W.; Ameringer, T.; Moeller, M. Ultrathin Coatings from Isocyanate Terminated Star PEG Prepolymers: Patterning of Proteins on the Layers. *Langmuir* **2005**, *21*, 3076−3083.
(45) Thiessen, M.; Abetz, V. Influence of the Glass Transition Temperature and the Density of Crosslinking Groups on the Reversibility of Diels-Alder Polymer Networks. *Polymers* **2021**, *13*, 1189.
(46) Wouters, M.; Craenmehr, E.; Tempelaars, K.; Fischer, H.; Stroeks, N.; van Zanten, J. Preparation and Properties of a Novel Remendable Coating Concept. *Prog. Org. Coat.* **2009**, *64*, 156−162.
(47) Engel, T.; Kickelbick, G. Self-Healing Nanocomposites from Silica − Polymer Core − Shell Nanoparticles. *Polym. Int.* **2014**, *63*, 915−923.
(48) Ruiz-Soria, G.; Pérez Paz, A.; Sauer, M.; Mowbray, D. J.; Lacovig, P.; Dalmiglio, M.; Lizzit, S.; Yanagi, K.; Rubio, A.; Goldoni, A.; Ayala, P.; Pichler, T. Revealing the Adsorption Mechanisms of Nitroxides on Ultrapure, Metallicity-Sorted Carbon Nanotubes. *ACS Nano* **2014**, *8*, 1375−1383.
(49) Couto, D.; Richter, A.; Walter, H.; Furkert, D.; Hothorn, M.; Fiedler, D. Using Biotinylated Myo-Inositol Hexakisphosphate to Investigate Inositol Pyrophosphate−Protein Interactions with Surface-Based Biosensors. *Biochemistry* **2021**, *60*, 2739−2748.
(50) Canalle, L. A.; Löwik, D. W. P. M.; van Hest, J. C. M. Polypeptide−Polymer Bioconjugates. *Chem. Soc. Rev.* **2010**, *39*, 329−353.
(51) Branco, M.; Caseiro, A. R.; Silva, D. M.; Amorim, I.; Rêma, A.; Pedrosa, S. S.; Branquinho, M. V.; Gomes, P. S.; Fernandes, M. H.; Santos, J. D.; Mauricio, A. C.; Sencadas, V. Processing, Characterization, and in Vivo Evaluation of Poly(L-lactic acid)-Fish Gelatin Electrospun Membranes for Biomedical Applications. *ACS Appl. Bio Mater.* **2018**, *1*, 226−236.
(52) Majidi, S. S.; Slemming-Adamsen, P.; Hanif, M.; Zhang, Z.; Wang, Z.; Chen, M. Wet Electrospun Alginate/Gelatin Hydrogel Nanofibers for 3D Cell Culture. *Int. J. Biol. Macromol.* **2018**, *118*, 1648−1654.
(53) Ma, C.; Choi, J.-B.; Jang, Y.-S.; Kim, S.-Y.; Bae, T.-S.; Kim, Y.-K.; Park, J.-M.; Lee, M.-H. Mammalian and Fish Gelatin Methacryloyl−Alginate Interpenetrating Polymer Network Hydrogels for Tissue Engineering. *ACS Omega* **2021**, *6*, 17433−17441.
(54) Yoon, H. J.; Shin, S. R.; Cha, J. M.; Lee, S.-H.; Kim, J.-H.; Do, J. T.; Song, H.; Bae, H. Cold Water Fish Gelatin Methacryloyl Hydrogel for Tissue Engineering Application. *PLoS One* **2016**, *11*, No. e0163902.
(55) Lerman, M. J.; Lembong, J.; Muramoto, S.; Gillen, G.; Fisher, J. P. The Evolution of Polystyrene as a Cell Culture Material. *Tissue Eng., Part B* **2018**, *24*, 359−372.
(56) Faussner, A.; Deininger, M. M.; Weber, C.; Steffens, S. Direct Addition of Poly-Lysine or Poly-Ethylenimine to the Medium: A Simple Alternative to Plate Pre-Coating. *PLoS One* **2022**, *17*, No. e0260173.
(57) Liberio, M. S.; Sadowski, M. C.; Soekmadji, C.; Davis, R. A.; Nelson, C. C. Differential Effects of Tissue Culture Coating Substrates on Prostate Cancer Cell Adherence, Morphology and Behavior. *PLoS One* **2014**, *9*, No. e112122.
(58) Ge, H.; Tan, L.; Wu, P.; Yin, Y.; Liu, X.; Meng, H.; Cui, G.; Wu, N.; Lin, J.; Hu, R.; Feng, H. Poly-L-Ornithine Promotes Preferred Differentiation of Neural Stem/Progenitor Cells Via Erk Signalling Pathway. *Sci. Rep.* **2015**, *5*, 15535.
(59) Klim, J. R.; Li, L.; Wrighton, P. J.; Piekarczyk, M. S.; Kiessling, L. L. A Defined Glycosaminoglycan-Binding Substratum for Human Pluripotent Stem Cells. *Nat. Methods* **2010**, *7*, 989−994.
(60) Burridge, P. W.; Matsa, E.; Shukla, P.; Lin, Z. C.; Churko, J. M.; Ebert, A. D.; Lan, F.; Diecke, S.; Huber, B.; Mordwinkin, N. M.; Plews, J. R.; Abilez, O. J.; Cui, B.; Gold, J. D.; Wu, J. C. Chemically Defined Generation of Human Cardiomyocytes. *Nat. Methods* **2014**, *11*, 855−860.
(61) Milky, B.; Zabolocki, M.; Al-Bataineh, S. A.; van den Hurk, M.; Greenberg, Z.; Turner, L.; Mazzachi, P.; Williams, A.; Illeperuma, I.; Adams, R.; Stringer, B. W.; Ormsby, R.; Poonnoose, S.; Smith, L. E.; Krasowska, M.; Whittle, J. D.; Simula, A.; Bardy, C. Long-Term Adherence of Human Brain Cells in Vitro Is Enhanced by Charged Amine-Based Plasma Polymer Coatings. *Stem Cell Rep.* **2022**, *17*, 489−506.

https://doi.org/10.1021/acs.chemmater.3c00225
Chem. Mater. XXXX, XXX, XXX−XXX